Anatomical 3D Modeling of Upper Limb for Bio-impedance based Hand Motion Interpretation

Enver Salkim and Yu Wu
Department of Electronic and Electrical Engineering, University College London, Torrington Place, London WC1E 7JE, UK
e-mail: e.salkim@ucl.ac.uk; yu.wu.09@ucl.ac.uk

***Abstract*—Bio-impedance analysis (BIA) is a non-invasive way of assessing body compositions and has been recently used for hand motion interpretation using 'brute force' pattern recognition. To better promote BIA applications in human-machine interface, this paper develops an anatomically accurate 3D model towards a sound BIA recording strategy. The model is developed based on transient finite element analysis. It can be used for precise location of transcutaneous electrical stimulation to provide 3D current and potential distributions within the skin, fat, muscle, and bone layers of the upper arm, each defined by their dielectric properties. With the model, it is possible to investigate the impact of the electrode placement on the muscle when using, e.g., textile and flexible electrodes. As proof of concept for guiding the electrode placement, the electrical potential was simulated for two different electrode stimulation arrangements. The results showed that when the electrodes were shifted towards the upper arm, the electrical potential was reduced. This may be related to the anatomical layers' electric features and the distance of the electrode to the targeted muscle.**

Keywords—Bio-impedance analysis, human-machine interface, transient finite element, upper arm volume conductor

I. INTRODUCTION

Over 3 million people worldwide suffer from upper-limb loss, and this number is expected to double by 2050. Prostheses improve people's quality of life who suffer from upper-limb loss. However current myoelectric prostheses only offer limited degrees-of-freedom (DOF), far from achieving the human-like hand motion [1].

Surface electromyography (sEMG) is the human-machine interface (HMI) method used in myoelectric prostheses [1]–[3]. Despite offering high recognition accuracy, the acceptance of myoelectric prostheses remains low. The fundamental challenges relate to the electromyography signals. Signal amplitudes of only up to tens of mV with frequencies up to about 500 Hz, make recording susceptible to noise and low-frequency interference. sEMG has limited spatial resolution, and deep muscle activity in the forearm is challenging to record [4] and only a limited number of DOFs are recognized. Alternative non-invasive ways of recording raw bio-signals may provide further advancement in the field.

Bio-impedance analysis (BIA) is a non-invasive way of assessing body compositions. Similar to sEMG, electrodes are placed on the skin. Instead of recording spontaneous signals like sEMG, BIA injects a current and measures resulting voltage potentials. Such current induced voltage signals have a better signal-to-noise ratio (SNR) and are related to the body compositions that is underneath the electrodes. BIA for HMI has been recently reported in [5], [6]. In such an HMI system, the forearm is surrounded by a flexible band containing an array of evenly distributed electrodes. As muscle and bone move inside the arm region enclosed by the band, the collected BIA dataset is then 'brute force' analysed to reflect upper limb movement using e.g., a machine learning algorithm.

However, to further promote the BIA in HMI towards a dexterous prosthesis, an optimized BIA recording strategy is required. This paper develops an anatomically accurate human arm model that can be used to investigate the impact of the electrode placement on the muscle for optimal and targeted BIA recording strategy using e.g., textile and flexible

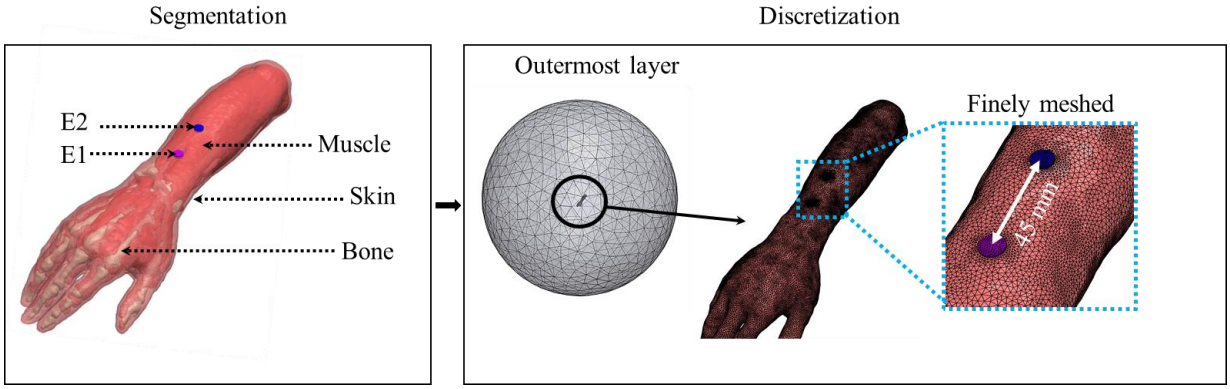

Fig. 1. The anatomical layers are segmented, and 3D domains are constructed based on the Duke model with associated labeling and smoothing filters in ScanIP software. The outermost layers are defined as a sphere model to imitate as the ground at infinity. The electrode is relatively finely meshed to obtain more accurate results.

This work was supported by the Engineering and Physical Sciences Research Council under grant EP/S032045/1.

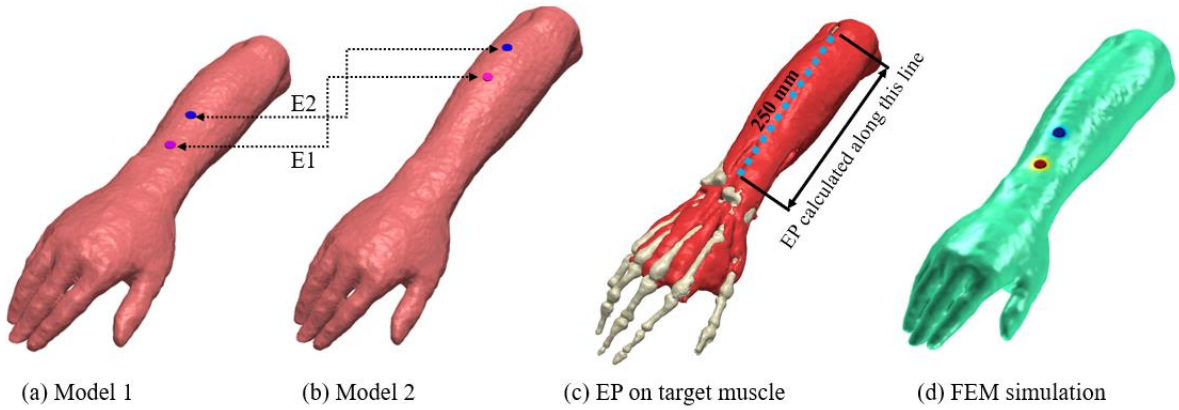

Fig. 2. (a) and (b) shows two different electrode models arrangement placed on the upper arm, for current stimulation, E1/2 represents electrodes; (c) the electrical potential (EP) was calculated along the selected muscle length marked by the dotted line; (d) the finite element method (FEM) simulation with the appropriate boundary condition and attained electrical parameters defined.

electrode arrays. The models are implemented in finite element (FE) models (FEM) involving a volume conductor model representing various anatomical structures and the electrodes by their respective dielectric features and appropriate boundary conditions [7]. The model allows ready investigation of the impact regarding electrode position using BIA.

The paper is organized as follows. Section II presents the method used to develop the model; Section III gives the results of chosen BIA simulation and the discussion and conclusion are given in Section IV and V, respectively.

Table 1. Tissue conductivities

Tissue layer	Conductivity (S/m)	Relative permittivity (F/m)
Skin	$1.7e-4$	$1.4e3$
Muscle (longitudinal)	0.315	$1.2e5$
Muscle (transverse)	0.105	$4e4$
Bone	0.02	$3e3$
Outermost Sphere	10^{-12}	1

II. METHODS

A. Human Arm Model Development

A realistic three-dimensional (3D) volume conductor model of the human arm was constructed from the Duke model v.2.0.1, of a healthy adult male subject [8]. Each tissue layer was imported from a library of Standard Tessellation Language (STL) surface triangulations of human anatomical parts. Since the Duke model consists of all tissue layers, it was focused on the region of interest to reduce computation cost. The arm model was derived using Boolean operations to provide a 3D model of the arm. The model is composed of the fundamental tissue layers of skin, muscles, and bones. The STL models were converted to the image data to generate a 3D model using image segmentation. The process of segmentation entails the identification and labeling of 'regions of interest' (ROIs) (e.g., skin, muscles, and bones) within the greyscale data, creating masks [7], [9]. Each mask is then segmented using automatic and manual segmentation processes in Simpleware ScanIP v2016.09 (Synopsys, Mountain View, USA), as shown in Fig. 1. Image filters were used on the masks to smooth these layers (recursive Gaussian, median, and mean filters), edit the morphology, or fill the cavities (dilate, erode, open and close functions). Lastly, Boolean operations were applied to obtain appropriate boundaries and remove any overlapping sections between the tissue layers.

B. Electrode Modelling and Boundary Conditions

The electrodes were defined as equipotential surfaces from which the current density distribution was nonuniform. The electrodes were designed based on smooth geometric shapes (e.g., cylinder) in Scan IP software to prevent any meshing problems. The radius of each electrode was set to 5 mm. The pitch of electrodes was chosen as 45 mm, as shown in Fig. 1. Two different electrode arrangements were designed and merged with the 3D arm model shown in Fig. 2. In all the simulated cases, the stimulation current was set up to 3 mA injected from the electrodes E1 (pink) and received from the return electrodes E2 (blue). The simulation was implemented in COMSOL Multiphysics v5.2a (COMSOL, Ltd, Cambridge, UK) by *Terminal* current negative for the cathodes and positive for the anodes. A square-wave current pulse with a pulse duration of 10 µs and different current amplitudes (from 1 mA_{peak} to 3 mA_{peak}) was applied to the electrodes for each model. The electrode-tissue interface contact impedance was assumed zero for simplicity reasons. A comparatively large non-conductive (σ = 10e-12 S/m) sphere was defined as the external boundary, and the Dirichlet boundary condition (V = 0) was applied, which was considered an approximation of the ground at infinity as shown in Fig. 1. (Note: appropriate continuity conditions were implemented at the boundaries of different media to obtain accurate solution.)

C. Finite Element Simulation

According to Maxwell's equations, the current and voltage vectors for arbitrary directions within a volume conductor can be calculated using the FEM. The FEM model of the upper arm was generated, and the simulations can be carried out using COMSOL based on the transient approximation of Maxwell equation (1) shown below:

$$\nabla \cdot \left(\sigma \nabla V - \varepsilon_0 \varepsilon_r \nabla \frac{\partial V}{\partial t}\right) \quad (1)$$

where σ is the low frequency conductivity of each of the tissues (i.e., considered with no frequency dependent elements), V is the electrical potential in the representative geometry, $\varepsilon_0\varepsilon_r$ is the tissue permittivity. In this work, to serve as a starting point for muscle targeting using BIA, the electrical properties used for the tissues are given in Table 1 [10]. The wave propagation and inductive effects were assumed to be negligible [9].

The model domain was discretized using the tetrahedral finite elements with the partial differential equations in COMSOL to solve the numerical solutions. In FEM modeling, the mesh elements need to be discretized small enough to ensure an accurate solution. The mesh-size was refined until no significant change could be found in the transient solution. Since the model comprises fundamental tissue layers, the domains can be meshed with finer discretization settings to obtain optimum mesh quality (without increasing computation cost significantly). The number of tetrahedral finite elements was about 1.5 million (about 1.8 million degrees of freedom), and the simulation time was approximately 20 minutes. Once the anatomical upper arm volume conductor model and electrode array settings are completed, each tissue layer's electrical characteristics (as shown in Table 1) are assigned to perform the electrical potential measurements. Each layer was described using conductivity and relative permittivity. It is noted that the anisotropic conductivity of a muscle was considered using the diagonal matrix of the conductivity.

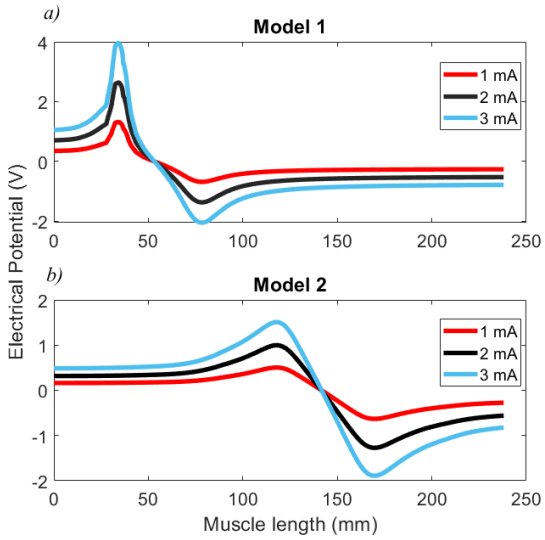

Fig. 3. a) The electrical potential (EP) variations versus the selected muscle length marked by the dotted line shown in Fig. 2 for model 1 electrode arrangement and b) model 2 electrode arrangement with different level of current injections.

III. RESULTS

The electrical potential (the peak voltage value) variation along the targeted muscle length (as marked by the dotted line in Fig. 2) is shown in Fig. 3. The results showed that the electrical potential variation is proportional to injected current levels. The induced electrical potential along the muscle length is relatively higher for model 1 electrode arrangement compared to model 2. At 3 mA current injection, the maximum voltage value is 4 V for model 1, and this is about 1.6 V for model 2 at the point of E1 electrode. After a certain muscle length after E1, the electrical potential is decreased to zero levels due to the existing of cathode (the E2 electrode) in the volume conductor for both models. It is also noted that the induced electrical potentials on the muscle length at E2 electrode position is at a similar level for both models, around -2 V.

IV. DISCUSSION

Bio-computational models can be used in the design and development of biomedical devices. Specifically, the electrode arrangement placement within the anatomical layer can be readily investigated using these models. The electrical potential is simulated within the volume conductor using appropriate boundary conditions and with attained associated tissue and electrode electrical parameters in such models. These models have been used in a variety of applications [7], [11],[12].

In this study, transient FE models were developed to simulate the electrical scalar potential's evolution inside the human body. The potential electrical distribution for two-electrode models placed on the human upper arm was simulated, and results were recorded. It was shown that the electrode's placement along the upper arm is vital based on electrical potential distribution along the selected muscle length. It was noted that this variation for model 1 was relatively higher when compared to model 2. This may be due to the difference between the electrical parameters of the skin and muscle layers. Also, the thickness of the skin is not constant along with the muscle. Thus, electrical potential distribution on the muscle may be higher at lower thickness.

Overall, more detailed electrode features (e.g., size, shape, gap) parameterization are required to analyse the different electrode impacts on BIA using sophisticated upper arm models. The results in Fig. 3 which include surrounding tissues, show a useful difference in electrical potential distributions with electrode models. This suggests that the placement of the electrode variations in impedance can be vital for induced electric potential on the target muscle.

V. CONCLUSION

In this study, the multilayer FEM models of the human arm were developed to investigate the impact of electrode placement on electric potential distribution along the selected muscle. As proof of concept, the electrical potential was simulated for two different electrode stimulation arrangements. The results showed that the electrical potential decreases as the electrode is shifted towards the upper arm. This may be related to the anatomical layers' electric features and the electrode's distance to the muscle. With further optimization, the model can be used to investigate the impact regarding electrode position for guiding, e.g., large-scale flexible printed electrode placement in BIA.

REFERENCES

[1] A. Fougner, O. Stavdahl, P. J. Kyberd, Y. G. Losier, and P. A. Parker, “Control of upper limb prostheses: Terminology and proportional myoelectric controla review,” IEEE Trans. Neural Syst. Rehabil. Eng., vol. 20, no. 5, pp. 663–677, 2012.

[2] G. Huang, Z. Zhang, D. Zhang, and X. Zhu, “Spatio-spectral filters for low-density surface electromyographic signal classification,” Med. Biol. Eng. Comput., vol. 51, no. 5, pp. 547–555, 2013.

[3] C. Cipriani et al., “Online myoelectric control of a dexterous hand prosthesis by transradial amputees,” IEEE Trans. Neural Syst. Rehabil. Eng., vol. 19, no. 3, pp. 260–270, 2011.

[4] P. F. Pasquina et al., “First-in-man demonstration of a fully implanted myoelectric sensors system to control an advanced electromechanical prosthetic hand,” J. Neurosci. Methods, vol. 244, pp. 85–93, 2015.
[5] Y. Zhang and C. Harrison, “Tomo: Wearable, Low-Cost, Electrical Impedance Tomography for Hand Gesture Recognition,” Proc. 28th Annu. ACM Symp. User Interface Softw. Technol. - UIST ’15, pp. 167–173, 2015.
[6] Y. Wu, D. Jiang, X. Liu, R. Bayford, and A. Demosthenous, “A Human-Machine Interface Using Electrical Impedance Tomography for Hand Prosthesis Control,” IEEE Trans. Biomed. Circuits Syst., vol. 12, no. 6, pp. 1322–1333, 2018.
[7] E. Salkim, A. Shiraz, and A. Demosthenous, “Impact of neuroanatomical variations and electrode orientation on stimulus current in a device for migraine: A computational study,” J. Neural Eng., vol. 17, no. 1, 2020.
[8] A. Christ et al., “The Virtual Family - Development of surface-based anatomical models of two adults and two children for dosimetric simulations,” Phys. Med. Biol., vol. 55, no. 2, 2010.
[9] E. Salkim, A. Shiraz, and A. Demosthenous, “Influence of cellular structures of skin on fiber activation thresholds and computation cost In fl uence of cellular structures of skin on fi ber activation thresholds and computation cost,” Biomed. Phys. Eng. Express, vol. 5, no. 1, p. 015015, 2018.
[10] C. Gabriel et al., “The dielectric properties of biological tissues: I. Literature survey,” Phys. Med. Biol., vol. 41, no. 11, pp. 2231–2249, Nov. 1996.
[11] K. Zhu, L. Li, X. Wei, and X. Sui, “A 3D computational model of transcutaneous electrical nerve stimulation for estimating Aß tactile nerve fiber excitability,” Front. Neurosci., vol. 11, no. MAY, 2017.
[12] A. Kuhn and T. Keller, “A 3d transient model for transcutaneous functional electrical stimulation,” Int. Funct. Electr. Stimul. Soc. Conf., vol. 10, no. July, pp. 385–7, 2005.